DOE/NASA/16310-11
NASA TM-102307

IN-26
231741
21P.

Creep Behavior of Tungsten Fiber Reinforced Niobium Metal Matrix Composites

T.L. Grobstein
National Aeronautics and Space Administration
Lewis Research Center

Work performed for
U.S. DEPARTMENT OF ENERGY
Nuclear Energy
Reactor Systems Development and Technology

Prepared for the
Sixth Symposium on Space Nuclear Power Systems
sponsored by the Institute for Space Nuclear Power Studies
Albuquerque, New Mexico, January 8–12, 1989

(NASA-TM-102307) CREEP BEHAVIOR OF TUNGSTEN FIBER REINFORCED NIOBIUM METAL MATRIX COMPOSITES Final Report (NASA. Lewis Research Center) 21 p CSCL 11F
N89-29522
Unclas
63/26 0231741

DISCLAIMER

This report was prepared as an account of work sponsored by an agency of the United States Government. Neither the United States Government nor any agency thereof, nor any of their employees, makes any warranty, express or implied, or assumes any legal liability or responsibility for the accuracy, completeness, or usefulness of any information, apparatus, product, or process disclosed, or represents that its use would not infringe privately owned rights. Reference herein to any specific commercial product, process, or service by trade name, trademark, manufacturer, or otherwise, does not necessarily constitute or imply its endorsement, recommendation, or favoring by the United States Government or any agency thereof. The views and opinions of authors expressed herein do not necessarily state or reflect those of the United States Government or any agency thereof.

Printed in the United States of America

Available from
National Technical Information Service
U.S. Department of Commerce
5285 Port Royal Road
Springfield, VA 22161

NTIS price codes[1]
Printed copy: A03
Microfiche copy: A01

[1]Codes are used for pricing all publications. The code is determined by the number of pages in the publication. Information pertaining to the pricing codes can be found in the current issues of the following publications, which are generally available in most libraries: *Energy Research Abstracts (ERA)*; *Government Reports Announcements and Index (GRA and I)*; *Scientific and Technical Abstract Reports (STAR)*; and publication, NTIS-PR-360 available from NTIS at the above address.

DOE/NASA/16310-11
NASA TM-102307

Creep Behavior of Tungsten Fiber Reinforced Niobium Metal Matrix Composites

T.L. Grobstein
National Aeronautics and Space Administration
Lewis Research Center
Cleveland, Ohio 44135

Work performed for
U.S. DEPARTMENT OF ENERGY
Nuclear Energy
Reactor Systems Development and Technology
Washington, D.C. 20545
Under Interagency Agreement DE-AI03-86SF16310

Prepared for the
Sixth Symposium on Space Nuclear Power Systems
sponsored by the Institute for Space Nuclear Power Studies
Albuquerque, New Mexico, January 8-12, 1989

CREEP BEHAVIOR OF TUNGSTEN FIBER REINFORCED NIOBIUM METAL MATRIX COMPOSITES

T. L. Grobstein
National Aeronautics and Space Administration
Lewis Research Center
Cleveland, Ohio 44135-3191

SUMMARY

Tungsten fiber reinforced niobium metal matrix composites were evaluated for use in space nuclear power conversion systems. The composite panels were fabricated using the arc-spray monotape technique at the NASA Lewis Research Center. The creep behavior of W/Nb composite material was determined at 1400 and 1500 K in vacuum over a wide range of applied loads. The time to reach 1% strain, the time to rupture, and the minimum creep rate were measured. The W/Nb composites exceeded the properties of monolithic niobium alloys significantly even when compared on a strength to density basis. The effect of fiber orientation on the creep strength also was evaluated. Kirkendall void formation was observed at the fiber/matrix interface; the void distribution differed depending on the fiber orientation relative to the stress axis. A relationship was found between the fiber orientation and the creep strength.

INTRODUCTION

Advanced materials will play a major role in meeting the stringent size and performance requirements of future space power systems. The requirements for such a system, which may include a service life of greater than 7 years at a temperature in excess of 1350 K, in addition to resistance to liquid metal corrosion, dictate the use of refractory metals. Currently, monolithic niobium-based alloys are specified for components in the power conversion system of space nuclear power systems. These include the niobium-1% zirconium alloy (Nb-1Zr) and the PWC-11 alloy (Nb-1Zr-0.1C). Tungsten fiber reinforced niobium metal matrix composites (W/Nb) are being considered for future applications in this area where higher temperature and higher stress conditions may exist. W/Nb composites offer potential for high tensile and creep strength applications up to 1700 K (Westfall et al 1986; Petrasek and Titran 1988).

One challenge to overcome in using these composites is the possible degradation in properties at long times due to interdiffusion between the fibers and matrix. Interdiffusion between tungsten and niobium results in a continuous solid solution and therefore would not be a catastrophic process, as it would be if a brittle intermetallic phase were formed. Interdiffusion may, however, cause recrystallization of the tungsten fibers which would reduce the strength of these fibers. The projected life (greater than 60 000 h) and temperature requirements (up to 1700 K) could therefore result in a reduction in creep strength of the W/Nb composite (Grobstein 1989).

MATERIALS AND PROCEDURE

The strength to density ratio of several tungsten-based wires compared to the Nb-1Zr alloy is plotted in Figure 1. Each of these wires has the potential for fiber reinforcement of the Nb-1Zr matrix due to their high strength. The weakest wire shown here is the 218CS wire, a potassium-doped commercially available lamp filament. The ST300 wire contains a fine dispersion of 1.5 wt% ThO_2, about 1 μm in size. The strongest wire contains an even finer dispersion of HfC particles. Photomicrographs of these three types of wire are shown in Figure 2. Unfortunately, the WHfC wire is not currently available, so the ST300 wire, with a diameter of 200 μm, was chosen for the reinforcement material.

The matrix materials were niobium and niobium with 1% zirconium. The addition of 1% zirconium to niobium results in zirconia precipitates which strengthen the alloy and removes oxygen from the grain boundaries of the niobium, which is important for lithium corrosion resistance. Niobium was chosen as a matrix material only for comparison purposes.

These composites were fabricated by the Lewis-patented arc-spray monotape technique (Westfall 1985). This process, schematized in Figure 3, consists of wrapping the reinforcing fibers on a drum, placing the drum in an air-tight chamber, evacuating the chamber, and back-filling it with argon. Next, two wires of the matrix composition are brought together in the arc-spray gun, an arc is struck between them, and pressurized argon blows the molten matrix material onto the reinforcing fibers. The drum rotates until all the fibers are covered; the resulting structure is a "monotape" consisting of one layer of fibers in a matrix (Figure 4). Layers of monotapes then can be hot pressed

or hot isostatically pressed (HIP), producing a fully densified consolidated structure with negligible fiber/matrix interfacial reaction (Figure 5). Composites panels can be fabricated with a wide range of fiber volume fractions and angle plies using this technique. In addition, tubing is easily made using monotapes (Figure 6).

Composites panels were fabricated having ~30 to 54 volume percent fibers. For comparison purposes, applied creep stresses were normalized to 50 volume percent using the equation,

$$\frac{\sigma_{app}}{v\%} = \frac{\sigma_{norm}}{50v\%}$$

Creep specimens having a gauge section 25 mm long and 6.35 mm wide were then electric discharge machined from the composite panels (Figure 7). The fibers in the specimens were oriented unidirectionally either parallel or perpendicular to the longitudinal specimen axis. Some specimens also were fabricated with fibers angle-plied ±15° to the longitudinal axis, as shown in Figure 8.

Creep-rupture tests were conducted in a vacuum of 7 $x10^{-5}$ MPa. Creep strains were measured optically via a cathetometer clamped to the furnace chamber frame sighting on Knoop hardness impressions placed 25 mm apart on the gauge length. The precision of creep strain measurements was estimated to be ~0.02% for the gauge length used. The strain on loading was measured and was incorporated in the reported total creep strain. Creep rupture data was obtained at 1400 and 1500 K.

RESULTS AND DISCUSSION

The fiber/matrix interfacial reaction was examined by metallographically polishing transverse sections of creep specimens. Figure 9a shows a ST300/Nb-1Zr composite which was under stress at 1500 K for ~2550 h. The distinct reaction zone appears to be a result of interdiffusion between the fiber and matrix. In the case shown in Figure 9a, the reaction zone was ~10 μm in width, resulting in approximately a 20% decrease in the unaffected fiber area. Figure 9b shows a ST300/Nb-1Zr specimen tested at 1500 K for ~5353 h. In this case, the reaction zone increased to ~15 μm in width, a 28% decrease in the unaffected fiber area. (These values are for 200 μm diameter fibers; the percentages would increase for smaller diameter fibers and decrease for larger ones.) The measured reaction zone width for these long-term exposure samples agrees with that predicted by measuring the reaction in specimens exposed for shorter times.

Typical fracture surfaces are shown in Figure 10. The reaction zone was more extensive for specimens exposed for the longer times, as was the porosity in the matrix. No difference was apparent in the fracture ductility for the conditions shown, although some evidence of matrix oxidation was evident in samples exposed for over 5000 h.

The rupture time versus the normalized applied stress is plotted in Figure 11, and Figure 12 shows the minimum creep rates plotted versus the

normalized stress. Again, the longer-term creep data obtained in this study validate predictions made based on previous shorter-term data (Petrasek and Titran 1988).

Microhardness measurements across the interfacial region shown in Figure 13 reveal that the properties of the zone are between that of the fiber and the matrix. In specimens exposed for long times, oxidation appeared to increase the hardness of the matrix somewhat.

Figure 14 displays the rupture strength of the composite at 1500 K as the fiber orientation is varied from 0 to 90° with respect to the stress axis. Composite specimens with a 0° fiber orientation are obviously the strongest, whereas those with a 90° orientation are the weakest. The creep fracture morphology of the transverse specimens (90°) specimens indicated that failure occurred in the matrix rather than due to cleavage of the fibers or debonding between the fiber and the matrix.

Interdiffusion between tungsten and niobium forms a binary solid solution (Shunk 1969). However, the rate at which the two types of atoms diffuse is not the same. Experimental measurements have shown that the element with the lower melting point diffuses faster (Reed-Hill 1973). Thus, in this system, the niobium will diffuse into the tungsten fiber faster than tungsten diffuses out into the matrix. After extended exposure at temperature, the niobium matrix will suffer a loss of mass because it loses more atoms than it gains, while the tungsten gains in mass. This is called the Kirkendall effect. As a result of this mass transfer, the fiber wants to expand and the matrix wants

to shrink, but these dimensional changes are resisted by the bulk of the metal that lies outside the diffusion zone. The matrix is therefore placed under a tensile stress, and the fiber under a compressive stress. These stress fields may bring about plastic flow, with the resulting structural changes normally associated with plastic deformation and high temperatures; formation of substructures, recrystallization, and grain growth.

The interdiffusion therefore results in a recrystallized and tungsten-depleted area within the original fiber diameter. Since drawn tungsten fibers have been shown to have as high as five times the strength of recrystallized tungsten due to their fibrous grain structure (Yih and Wang 1979), this recrystallized interdiffusion zone may adversely affect the composite properties.

In addition to the effects listed above, the disparity in diffusion rates may cause Kirkendall void formation. Since there is a net vacancy flow in one direction, voids may form in the region of the diffusion zone from which there is a flow of mass. In the composite, this is just outside the fiber diameter. These type of voids are shown in Figure 15a. It should be noted that void formation may be influenced by necking of the fibers at failure, which will cause the fiber to pull away from the matrix. These tensile stresses and those due to mass flow are a contributing factor in the development of voids. Barnes and Mazey (1958) found that if this tensile stress is counteracted by a hydrostatic compressive stress placed on the sample, the voids can be prevented from forming.

Suppression of the void formation is observed in ±15° angle-plied composites in some areas around the fiber in Figure 15b. Compressive stresses are present parallel to the long transverse direction (vertical in this micrograph), so the Kirkendall voids form only in the unaffected areas. Similarly, void formation should be accelerated in specimens with transversely oriented fibers, although this was not observed in samples tested up to 800 h. Although the effect of fiber/matrix interdiffusion on properties does not appear to be significant from the results presented here, it is not yet fully understood. Consequently, the apparent loss in creep strength of samples with the longest times to rupture (Figures 11 and 12) was attributed to oxidation of the matrix rather than to interdiffusion zone effects.

Figure 16 compares the time to 1% strain of unidirectionally reinforced composites to ST300/Nb angle-plied composites, monolithic commercial Nb-1Zr, and the PWC-11 alloy (Nb-1Zr-0.1C). Composites with ±15° angle-plied fibers were ~20% weaker, but exhibited approximately the same stress exponent as the unidirectionally reinforced panels, indicating that the same creep mechanisms were at work. It is seen in this figure that the properties of even those panels with ±15° angle-plied fibers exceeded the creep properties of the monolithic PWC-11 alloy by a factor of four and the Nb-1Zr alloy by an order of magnitude.

CONCLUSIONS

1. The results presented here indicate that W/Nb composites have good potential for use in space power systems.

2. Angle-plying the reinforcing fibers has the potential to increase the transverse strength of the composite.

3. Interdiffusion between tungsten and niobium did not appear to significantly degrade the creep strength of the composite at times up to 5000 h.

4. The creep properties of W/Nb composites at 1500 K significantly exceeded those of monolithic niobium alloys even when compared on a strength to density basis.

Acknowledgements

Discussions with RH Titran and DW Petrasek were indispensable to the completion of this study. Expert metallography by TA Leonhardt is also gratefully acknowledged. This work was performed by the NASA Lewis Research Center for NASA and the Strategic Defense Initiative Office under an interagency agreement entered into in October 1985.

References

Barnes, R.S. and D.J. Mazey (1958) The Effect of Pressure Upon Void Formation in Diffusion Couples, Acta Met 6, pp 1-7.

Grobstein, T.L. (1989) The Interface in Tungsten Fiber Reinforced Niobium Metal Matrix Composites, PhD Thesis, Case Western Reserve University, Cleveland, OH.

Petrasek, D.W. (1972) High-Temperature Strength of Refractory-Metal Wires and Consideration for Composite Applications, NASA TN D-6881, NASA Lewis Research Center, Cleveland, OH.

Petrasek, D.W. and G. Beremand (1987) unpublished data, NASA Lewis Research Center, Cleveland, OH.

Petrasek, D.W. and R.A. Signorelli (1969) Stress-Rupture and Tensile Properties of Refractory-Metal Wires at 2000° and 2200°F (1093° and 1204°C, NASA TN D-5139, NASA Lewis Research Center, Cleveland, OH.

Petrasek, D.W. and R.H. Titran (1988) Creep Behavior of Tungsten/Niobium and Tungsten/Niobium - 1%Zirconium Composites, DOE/NASA-16310-5, NASA TM-100804, NASA Lewis Research Center, Cleveland, OH.

Reed-Hill, R.E. (1973) Physical Metallurgy Principles, D Van Nostrand Company, New York, NY, pp 386-392.

Shunk, F.A. (1969) Constitution of Binary Alloys, Second Supplement, McGraw-Hill Book Company, New York, NY, pp 209-210.

Tietz, T.E. and J.W. Wilson (1965) Behavior and Properties of Refractory Metals, Stanford University Press, Stanford, CA.

Titran, R.H., J.R. Stephans, and D.W. Petrasek (1988) Refractory Metal Alloys and Composites for Space Nuclear Power Systems, DOE/NASA/16310-8, NASA TM-101364, NASA Lewis Research Center, Cleveland, OH.

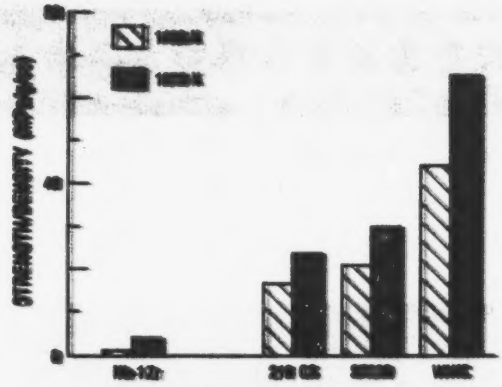

FIGURE 1. - COMPARISON OF THE 100-hr STRESS-RUPTURE STRENGTH TO DENSITY RATIO FOR THREE TUNGSTEN-BASED ALLOY WIRES COMPARED TO MONOLITHIC Mo-12Y ALLOY. (FROM TIETZ AND WILSON 1965; PETRASEK 1972; PETRASEK AND BERNARD 1987; PETRASEK AND SIEMERSMA 1988).

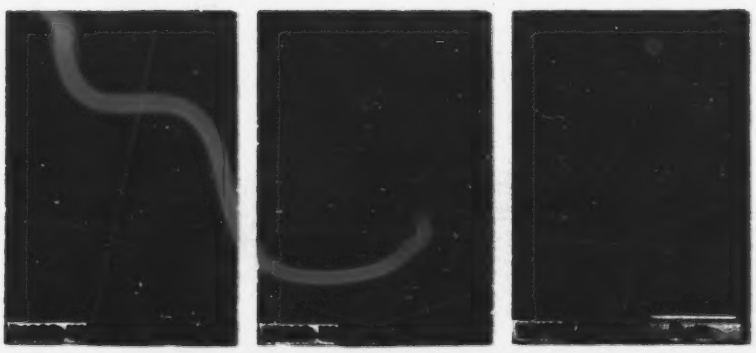

FIGURE 2. - LONGITUDINAL SECTIONS OF AS-DRAWN TUNGSTEN-BASED ALLOY WIRES. THE 218-CS WIRE IS A 200 μm FIBER DOPED WITH POTASSIUM. THE ST500 WIRE IS ALSO 200 μm DIAMETER WITH 1.5 wt % THORIA. THE WAC HAS A DIAMETER OF 375 μm WITH ~1 wt % HAFNIUM CARBIDE IN A FINE DISPERSION.

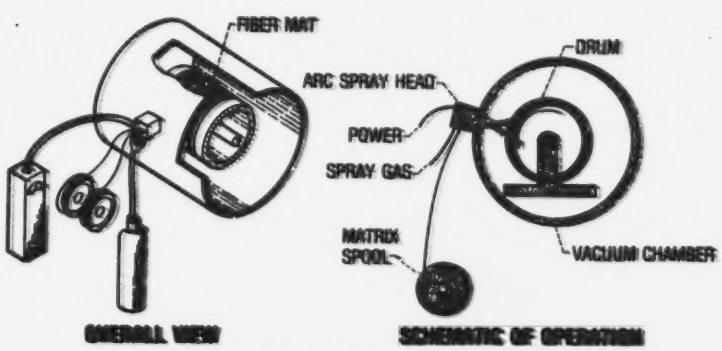

FIGURE 3. - SCHEMATIC OF THE ARC-SPRAY MONOTAPE FABRICATION PROCESS.

ORIGINAL PAGE
BLACK AND WHITE PHOTOGRAPH

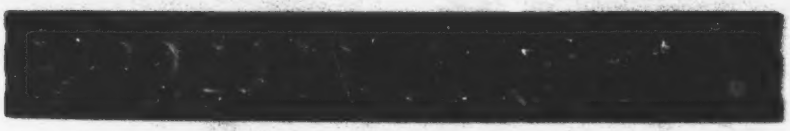

FIGURE 4. - MICROSTRUCTURE OF AN AS-GROWN RENIFORE.

FIGURE 5. - MICROSTRUCTURE OF AN AS-FABRICATED ST300/Nb COMPOSITE PANEL. CROSSHEADS. ~50 vol. % FIBER.

FIGURE 6. - W/Nb TUBE WITH THREE LAYERS OF FIBERS WITHIN A 15-mm OUTSIDE DIAMETER.

ORIGINAL PAGE
BLACK AND WHITE PHOTOGRAPH

FIGURE 7.- TYPICAL FRACTURED [illegible] CREEP SPECIMEN. TUNGSTEN WIRE, 10.5 μm DIAMETER WAS ELECTRON BEAM WELDED OVER THE ENDS OF THE SAMPLES TO PREVENT SHEAR PULLOUT OF THE FIBERS AT THE GRIPS.

ORIGINAL PAGE
BLACK AND WHITE PHOTOGRAPH

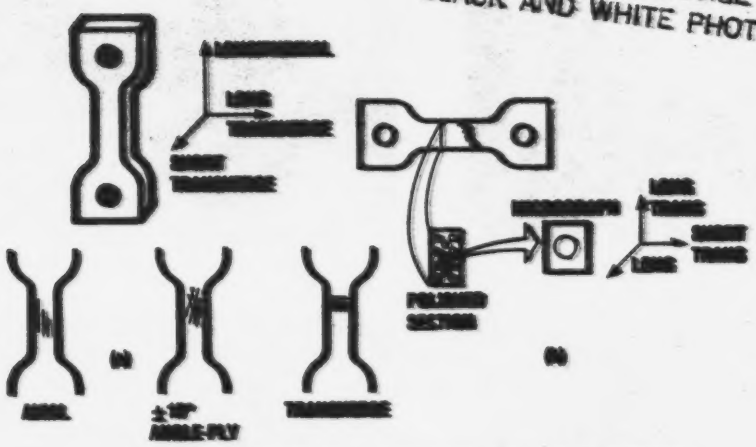

FIGURE 8. - SCHEMATIC OF THE FIBER ORIENTATIONS IN W/Nb CREEP SPECIMENS

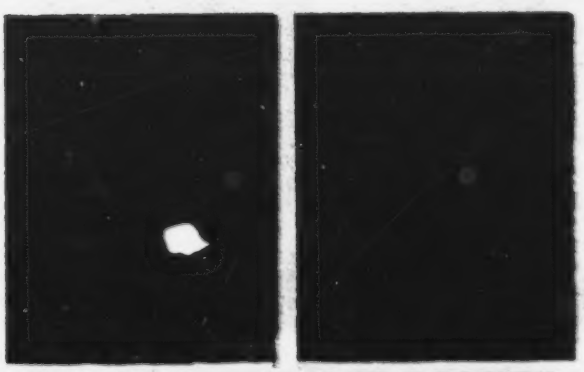

FIGURE 9. - TRANSVERSE SECTIONS OF W/Nb COMPOSITES CREEP TESTED AT 1500 K UNDER A NORMALIZED APPLIED STRESS OF (a) 107 MPa FOR 2500 h, AND (b) 80 MPa FOR 5057 h. METALLOGRAPHIC PREPARATION ILLUSTRATES THE REACTION ZONE BETWEEN THE FIBER AND MATRIX.

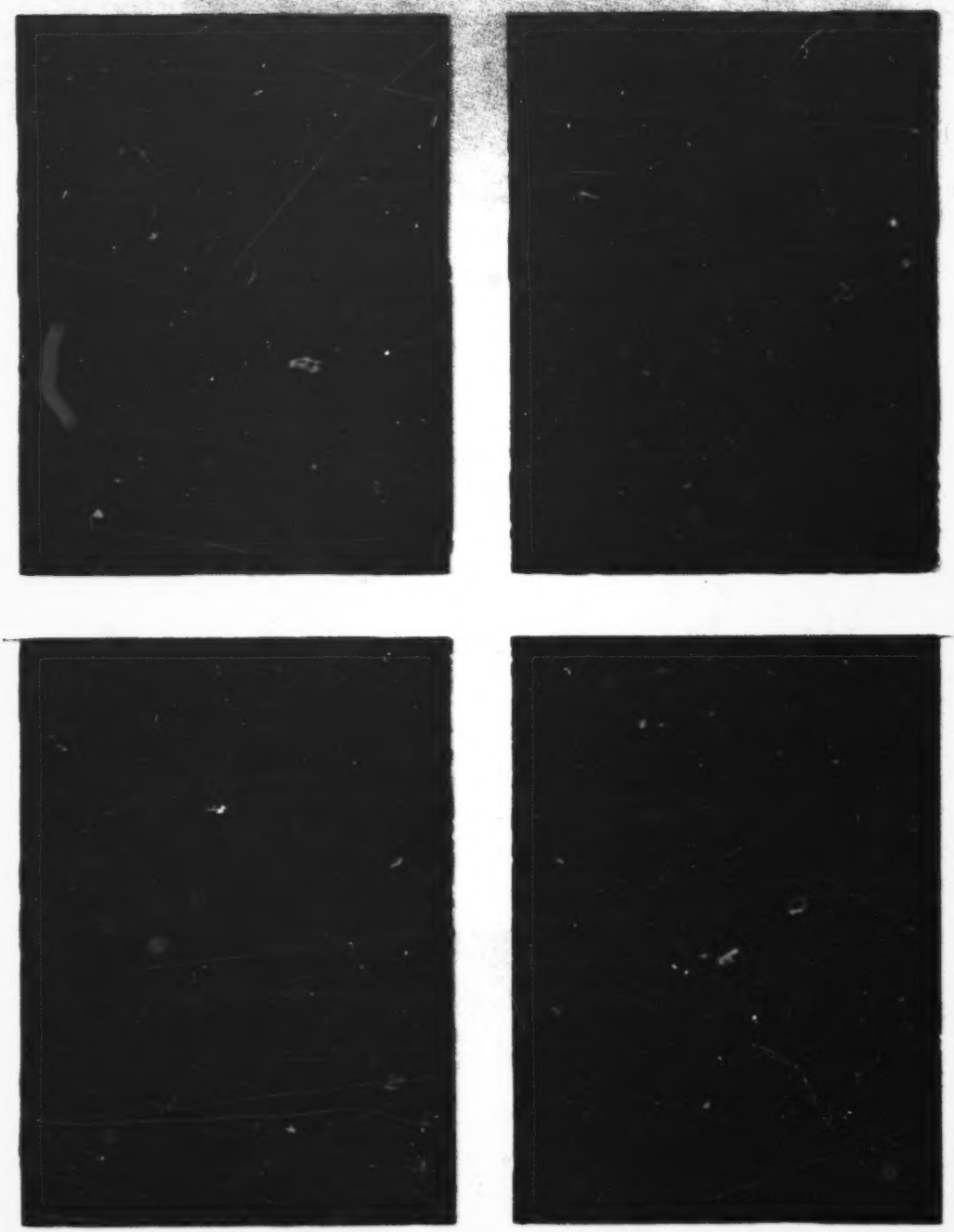

FIGURE 10. - FRACTURE SURFACES OF SiMo COMPOSITES CREEP TESTED AT 1500 K UNDER AN APPLIED STRESS OF (A) 220 MPa FOR 425 hr. (B) 80 MPa FOR 5353 hr. (C) 150 MPa FOR 597 hr. AND (D) 131 MPa FOR 2485 hr. SEM MICROGRAPHS REVEAL THE DIFFERENT FRACTURE MODES OF THE FIBER AND MATRIX.

ORIGINAL PAGE
BLACK AND WHITE PHOTOGRAPH

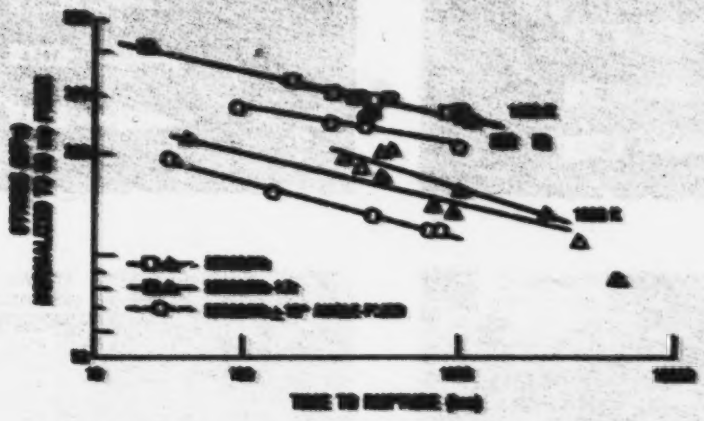

FIGURE 11. - TIME-TO-RUPTURE VERSUS THE NORMALIZED APPLIED STRESS (50 vol. % FP2 WHISKER COMPOSITES CREEP TESTED AT 1400 AND 1500 K.

FIGURE 12. - MINIMUM CREEP RATE VERSUS THE NORMALIZED APPLIED STRESS (50 vol. % FP2 WHISKER COMPOSITES CREEP TESTED AT 1400 AND 1500 K.

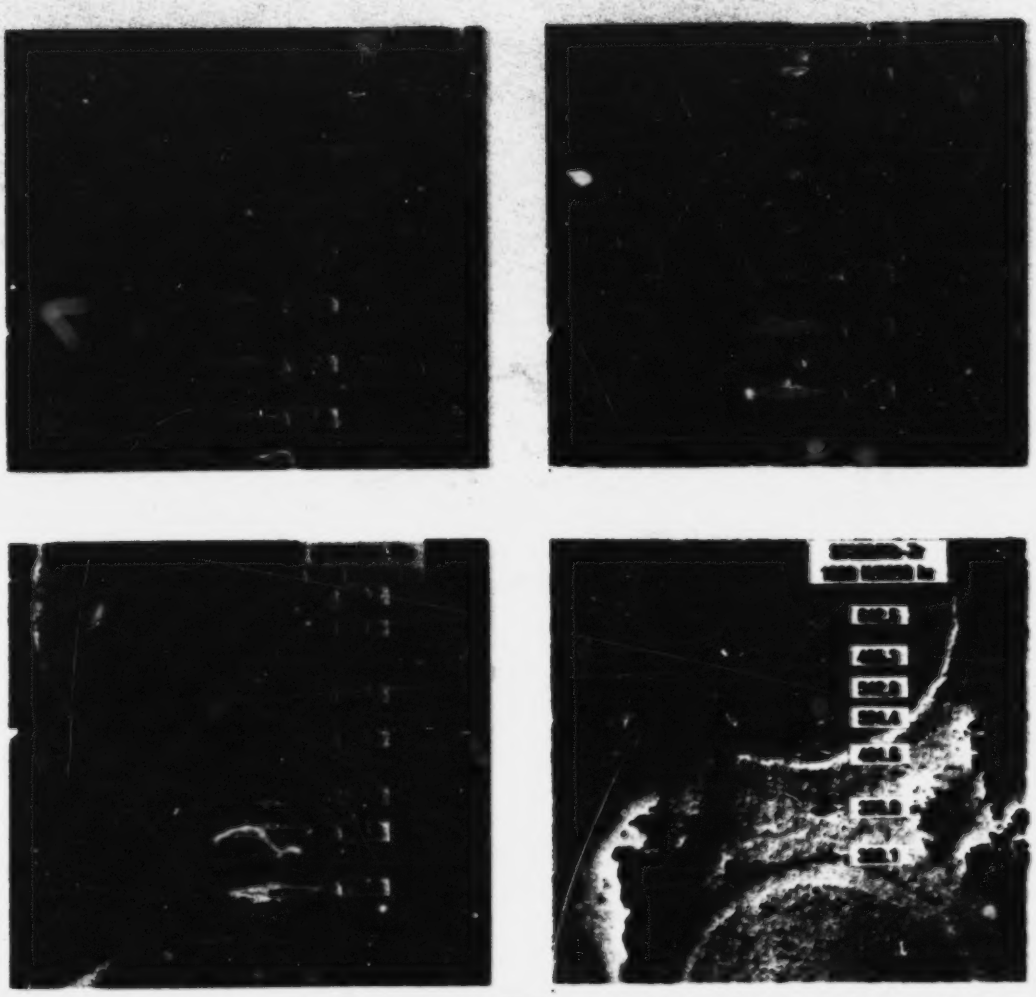

FIGURE 13. - MACROHARDNESS MEASUREMENTS OF COMPOSITE SECTIONS AFTER CREEP TESTING. UNITS ARE 10 KSI.

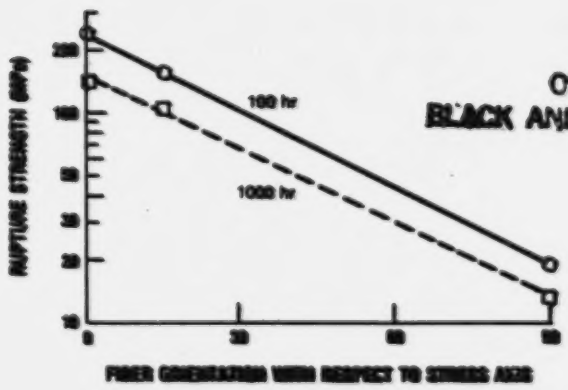

ORIGINAL PAGE
BLACK AND WHITE PHOTOGRAPH

FIBER ORIENTATION WITH RESPECT TO STRESS AXIS

FIGURE 14. - EFFECT OF FIBER ORIENTATION WITH RESPECT TO THE APPLIED STRESS ON THE RUPTURE STRENGTH OF SI3N4/Nb COMPOSITES AT 1500 K.

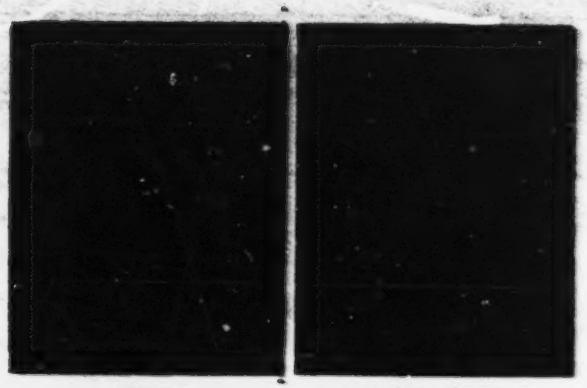

FIGURE 15. - TRANSVERSE SECTIONS IN THE AS-POLISHED CONDITION REVEAL THE PRESENCE OF VOIDS AT THE FIBER/MATRIX INTERFACE. THE MICROGRAPH IN (A) SHOWS A SINGLE FIBER IN A COMPOSITE PANEL WITH UNIDIRECTIONAL AXIAL REINFORCEMENT. THE MICROSTRUCTURE EXHIBITS A UNIFORM DISTRIBUTION OF VOIDS JUST OUTSIDE THE ORIGINAL FIBER DIAMETER. THE FIBERS IN THE PANEL IN (b) WERE ANGLE-PLIED ±15° TO THE LONGITUDINAL AXIS.

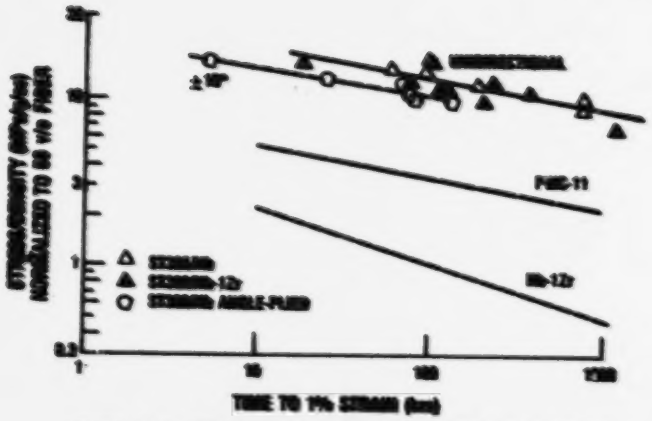

FIGURE 16. - COMPARISON OF THE TIME-TO-1%-STRAIN AT 1500 K FOR SCS6 TUNGSTEN FIBER REINFORCED COMPOSITES AND THE REFRACTORY Nb ALLOYS Nb-12Y AND PWC-11 (Nb-12Y-0.1C). (AFTER TITRAN ET AL., 1988). ALL DATA IS PLOTTED ON A STRESS TO DENSITY BASIS, AND THE COMPOSITE DATA WAS NORMALIZED TO 50 vol. % FIBER.

ORIGINAL PAGE
BLACK AND WHITE PHOTOGRAPH

Report Documentation Page

1. Report No.	2. Government Accession No.	3. Recipient's Catalog No.
NASA TM–102307 DOE/NASA/16310–11		

4. Title and Subtitle
Creep Behavior of Tungsten Fiber Reinforced Niobium Metal Matrix Composites

5. Report Date

6. Performing Organization Code

7. Author(s)
T.L. Grobstein

8. Performing Organization Report No.
E–4995

10. Work Unit No.
586–01–11

9. Performing Organization Name and Address
National Aeronautics and Space Administration
Lewis Research Center
Cleveland, Ohio 44135–3191

11. Contract or Grant No.

13. Type of Report and Period Covered
Technical Memorandum

12. Sponsoring Agency Name and Address
U.S. Department of Energy
Reactor Systems Development and Technology
Washington, D.C. 20545

14. Sponsoring Agency Code

15. Supplementary Notes
Final Report. Prepared under Interagency Agreement DE–AI03–86SF16310. Prepared for the Sixth Symposium on Space Nuclear Power Systems, sponsored by the Institute for Space Nuclear Power Studies, Albuquerque, New Mexico, January 8–12, 1989.

16. Abstract
Tungsten fiber reinforced niobium metal matrix composites were evaluated for use in space nuclear power conversion systems. The composite panels were fabricated using the arc-spray monotape technique at the NASA Lewis Research Center. The creep behavior of W/Nb composite material was determined at 1400 and 1500 K in vacuum over a wide range of applied loads. The time to reach 1-percent strain, the time to rupture, and the minimum creep rate were measured. The W/Nb composites exceeded the properties of monolithic niobium alloys significantly even when compared on a strength to density basis. The effect of fiber orientation on the creep strength also was evaluated. Kirkendall void formation was observed at the fiber/matrix interface; the void distribution differed depending on the fiber orientation relative to the stress axis. A relationship was found between the fiber orientation and the creep strength.

17. Key Words (Suggested by Author(s))
Tungsten alloys; Tungsten fibers; Niobium alloys; Metal matrix composites; Refractory metals; Mechanical properties; Creep-rupture; Fiber reinforcement

18. Distribution Statement
Unclassified–Unlimited
Subject Category 26
DOE Category UC–25

19. Security Classif. (of this report)	20. Security Classif. (of this page)	21. No of pages	22. Price*
Unclassified	Unclassified	18	A03

NASA FORM 1626 OCT 86

*For sale by the National Technical Information Service, Springfield, Virginia 22161